

Figure 6.42: The repeat unit of guaran, a naturally occurring polysaccharide, consisting of $(1 \rightarrow 4)$ - β -D-mannopyranosyl units with α -D-galactopyranosyl side chains attached to about every other mannose via $(1 \rightarrow 6)$ linkages.

The synthesis of a typical boric acid cross-linked guar gel, with viscosity properties suitable for use as a fracturing fluid, involves mixing guar gum, water and boric acid, $B(OH)_3$, in a 10:2000:1 wt/wt ratio. Adjusting the pH to between 8.5 and 9 results in a viscous gel. The boron:guaran ratio corresponds to almost 2 boron centers per 3 monosaccharide repeat units. Such a large excess of boric acid clearly indicates that the system is not optimized for cross-linking, i.e., a significant fraction of the boric acid is ineffective as a cross-linking agent.

The reasons for the inefficiency of boric acid to cross-link guaran (almost 2 borate ions per 3 monosaccharide repeat unit are required for a viscous gel suitable as a fracturing fluid): the most reactive sites on the component saccharides (mannose and galactose) are precluded from reaction by the nature of the guar structure; the comparable acidity (pK_a) of the remaining guaran alcohol substituents and the water solvent, results in a competition between cross-linking and borate formation; a significant fraction of the boric acid is ineffective in cross-linking guar due to the modest equilibrium (K_{eq}).

6.5.2.4 Bibliography

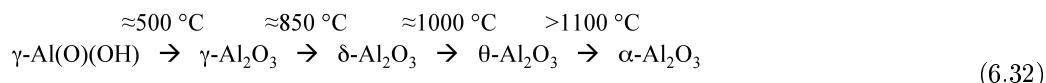
- F. A. Cotton and G. Wilkinson, *Advanced Inorganic Chemistry*, 4th Ed. Wiley Interscience (1980).
- M. Bishop, N. Shahid, J. Yang, and A. R. Barron, *Dalton Trans.*, 2004, 2621.
- M. Van Duin, J. A. Peters, A. P. G. Kieboom, and H. Van Bekkum, *Tetrahedron*, 1984, **40**, 2901.
- *Zonal Isolation*, "Borate Crosslinked Fluids," by R. J. Powell and J. M. Terracina, Halliburton, Duncan, OK (1998).
- R. Schechter, *Oil Well Stimulation*, Prentice-Hall Inc., Englewood Cliffs, NJ (1992).
- S. Kesavan and R. K. Prud'homme, *Macromolecules*, 1992, **25**, 2026.

6.5.3 Aluminum Oxides, Hydroxides, and Hydrated Oxides⁸

The many forms of aluminum oxides and hydroxides are linked by complex structural relationships. Bauxite has the formula $Al_x(OH)_{3-2x}$ ($0 < x < 1$) and is thus a mixture of Al_2O_3 (α -alumina), $Al(OH)_3$ (gibbsite), and $AlO(OH)$ (boehmite). The latter is an industrially important compound that is used in the form of a gel as a pre-ceramic in the production of fibers and coatings, and as a fire-retarding agent in plastics.

⁸This content is available online at <http://cnx.org/content/m32521/1.2/>.

Knowledge of microstructural evolution in ceramic systems is important in determining their end-use application. In this regard alumina has been the subject of many studies in which the phase, morphology, porosity and crystallinity are controlled by physical and chemical processing. The transformation from boehmite [γ -Al(O)(OH)] to corundum (α -Al₂O₃) has been well characterized and is known to go through the following sequence:



The phase changes from boehmite through θ -Al₂O₃ are known to be topotactic (i.e., changes in crystal structure are accomplished without changes in crystalline morphology), however, each phase change is accompanied by a change in porosity. The θ - to α -Al₂O₃ phase transition occurs through nucleation and growth of the θ -Al₂O₃ crystallites. The α -Al₂O₃ phase transition temperature can be altered by the addition of certain additives. For example, because the α -Al₂O₃ phase occurs by nucleation, the addition of small seed crystals can lower the transition temperature between 100 and 200 °C. The addition of certain transition metals (chromium, manganese, iron, cobalt, nickel, and copper) has also been shown to decrease the transition temperature, while lanthanum or rare earth metals tend to increase the temperature. Finally, the addition of metal oxides has also shown to affect the growth rate in α -Al₂O₃.

A third form of Al₂O₃ forms on the surface of the clean aluminum metal, (6.33). This oxide skin is rapidly self-repairing because its heat of formation is so large ($\Delta H = 3351$ kJ/mol). The thin, tough, transparent oxide layer is the reason for much of the usefulness of aluminum.



6.5.3.1 Bibliography

- K. Wefers and C. Misra, *Oxides and Hydroxides of Aluminum*, Alcoa Laboratories (1987).
- H. L. Wen and F. S. Yen, *J. Cryst. Growth*, 2000, **208**, 696.
- G. K. Priya, P. Padmaja, K. G. K. Warriar, A. D. Damodaran, and G. Aruldas, *J. Mater. Sci. Lett.*, 1997, **16**, 1584.
- E. Prouzet, D. Fargeot, and J. F. Baumard, *J. Mater. Sci. Lett.*, 1990, **9**, 779.

6.5.4 Ceramic Processing of Alumina⁹

6.5.4.1 Introduction

While aluminum is the most abundant metal in the earth's crust (ca. 8%) and aluminum compounds such as alum, K[Al(SO₄)₂].12(H₂O), were known throughout the world in ancient times, it was not until the isolation of aluminum in the late eighteenth century by the Danish scientist H. C. Ørsted that research into the chemistry of the Group 13 elements began in earnest. Initially, metallic aluminum was isolated by the reduction of aluminum trichloride with potassium or sodium; however, with the advent of inexpensive electric power in the late 1800's, it became economically feasible to extract the metal via the electrolysis of alumina (Al₂O₃) dissolved in cryolite, Na₃AlF₆, (the Hall-Heroult process). Today, alumina is prepared by the Bayer process, in which the mineral bauxite (named for Les Baux, France, where it was first discovered) is dissolved with aqueous hydroxides, and the solution is filtered and treated with CO₂ to precipitate alumina. With availability of both the mineral and cheap electric power being the major considerations in the economical production of aluminum, it is not surprising that the leading producers of aluminum are the United States, Japan, Australia, Canada, and the former Soviet Union.

⁹This content is available online at <<http://cnx.org/content/m22376/1.6/>>.

6.5.4.2 Aluminum oxides and hydroxides

The many forms of aluminum oxides and hydroxides are linked by complex structural relationships. Bauxite has the formula $\text{Al}_x(\text{OH})_{3-2x}$ ($0 < x < 1$) and is thus a mixture of Al_2O_3 (α -alumina), $\text{Al}(\text{OH})_3$ (gibbsite), and $\text{AlO}(\text{OH})$ (boehmite). The latter is an industrially important compound which is used in the form of a gel as a pre-ceramic in the production of fibers and coatings, and as a fire retarding agent in plastics.

Heating boehmite and diasporite to 450 °C causes dehydration to yield forms of alumina which have structures related to their oxide-hydroxide precursors. Thus, boehmite produces the low-temperature form γ -alumina, while heating diasporite will give α -alumina (corundum). γ -alumina converts to the hcp structure at 1100 °C. A third form of Al_2O_3 forms on the surface of the clean aluminum metal. The thin, tough, transparent oxide layer is the reason for much of the usefulness of aluminum. This oxide skin is rapidly self-repairing because its heat of formation is so large ($\Delta H = -3351 \text{ kJ/mol}$).



6.5.4.2.1 Ternary and mixed-metal oxides

A further consequence of the stability of alumina is that most if not all of the naturally occurring aluminum compounds are oxides. Indeed, many precious gemstones are actually corundum doped with impurities. Replacement of aluminum ions with trace amounts of transition-metal ions transforms the formerly colorless mineral into ruby (red, Cr^{3+}), sapphire (blue, $\text{Fe}^{2+/3+}$, Ti^{4+}), or topaz (yellow, Fe^{3+}). The addition of stoichiometric amounts of metal ions causes a shift from the α - Al_2O_3 hcp structure to the other common oxide structures found in nature. Examples include the perovskite structure for ABO_3 type minerals (e.g., CeTiO_7 or LaAlO_3) and the spinel structure for AB_2O_4 minerals (e.g., beryl, BeAl_2O_4).

Aluminum oxide also forms ternary and mixed-metal oxide phases. Ternary systems such as mullite ($\text{Al}_6\text{Si}_2\text{O}_{13}$), yttrium aluminum garnet (YAG, $\text{Y}_3\text{Al}_5\text{O}_{12}$), the β -aluminas (e.g., $\text{NaAl}_{11}\text{O}_{17}$) and aluminates such as hibonite ($\text{CaAl}_{12}\text{O}_{19}$) possessing β -alumina or magnetoplumbite-type structures can offer advantages over those of the binary aluminum oxides.

Applications of these materials are found in areas such as engineering composite materials, coatings, technical and electronic ceramics, and catalysts. For example, mullite has exceptional high temperature shock resistance and is widely used as an infrared-transparent window for high temperature applications, as a substrate in multilayer electronic device packaging, and in high temperature structural applications. Hibonite and other hexaluminates with similar structures are being evaluated as interfacial coatings for ceramic matrix composites due to their high thermal stability and unique crystallographic structures. Furthermore, aluminum oxides doped with an alkali, alkaline earth, rare earth, or transition metal are of interest for their enhanced chemical and physical properties in applications utilizing their unique optoelectronic properties.

6.5.4.3 Synthesis of aluminum oxide ceramics

In common with the majority of oxide ceramics, two primary synthetic processes are employed for the production of aluminum oxide and mixed metal oxide materials:

1. The traditional ceramic powder process.
2. The solution-gelation, or "sol-gel" process.

The environmental impact of alumina and alumina-based ceramics is in general negligible; however, the same cannot be said for these methods of preparation. As practiced commercially, both of the above processes can have a significant detrimental environmental impact.

6.5.4.3.1 Traditional ceramic processing

Traditional ceramic processing involves three basic steps generally referred to as powder-processing, shape-forming, and densification, often with a final mechanical finishing step. Although several steps may be energy intensive, the most direct environmental impact arises from the shape-forming process where various binders, solvents, and other potentially toxic agents are added to form and stabilize a solid ("green") body (Table 6.13).

Function	Composition	Volume (%)
Powder	alumina (Al ₂ O ₃)	27
Solvent	1,1,1-trichloroethane/ethanol	58
Deflocculant	menhaden oil	1.8
Binder	poly(vinyl butyrol)	4.4
Plasticizer	poly(ethylene glycol)/octyl phthalate	8.8

Table 6.13: Typical composition of alumina green body

The component chemicals are mixed to a slurry, cast, then dried and fired. In addition to any innate health risk associated with the chemical processing these agents are subsequently removed in gaseous form by direct evaporation or pyrolysis. The replacement of chlorinated solvents such as 1,1,1-trichloroethylene (TCE) must be regarded as a high priority for limiting environmental pollution. The United States Environmental Protection Agency (EPA) included TCE on its 1991 list of 17 high-priority toxic chemicals targeted for source reduction. The plasticizers, binders, and alcohols used in the process present a number of potential environmental impacts associated with the release of combustion products during firing of the ceramics, and the need to recycle or discharge alcohols which, in the case of discharge to waterways, may exert high biological oxygen demands in the receiving communities. It would be desirable, therefore, to be able to use aqueous processing; however, this has previously been unsuccessful due to problems associated with batching, milling, and forming. Nevertheless, with a suitable choice of binders, etc., aqueous processing is possible. Unfortunately, in many cast-parts formed by green body processing the liquid solvent alone consists of over 50 % of the initial volume, and while this is not directly of an environmental concern, the resultant shrinkage makes near net shape processing difficult.

6.5.4.3.2 Sol-gel

Whereas the traditional sintering process is used primarily for the manufacture of dense parts, the solution-gelation (sol-gel) process has been applied industrially primarily for the production of porous materials and coatings.

Sol-gel involves a four stage process: dispersion, gelation, drying, and firing. A stable liquid dispersion or *sol* of the colloidal ceramic precursor is initially formed in a solvent with appropriate additives. By changing the concentration (aging) or pH, the dispersion is "polymerized" to form a solid dispersion or *gel*. The excess liquid is removed from this gel by drying and the final ceramic is formed by firing the gel at higher temperatures.

The common sol-gel route to aluminum oxides employs aluminum hydroxide or hydroxide-based material as the solid colloid, the second phase being water and/or an organic solvent, however, the strong interactions of the freshly precipitated alumina gels with ions from the precursor solutions makes it difficult to prepare these gels in pure form. To avoid this complication, alumina gels are also prepared from the hydrolysis of aluminum alkoxides, Al(OR)₃.





The exact composition of the gel in commercial systems is ordinarily proprietary, however, a typical composition will include an aluminum compound, a mineral acid, and a complexing agent to inhibit premature precipitation of the gel, e.g., Table 6.14.

Function	Composition
Boehmite precursor	ASB [aluminum <i>sec</i> -butoxide, $\text{Al}(\text{OC}_4\text{H}_9)_3$]
Electrolyte	HNO_3 0.07 mole/mole ASB
Complexing agent	glycerol <i>ca.</i> 10 wt.%

Table 6.14: Typical composition of an alumina sol-gel for slipcast ceramics.

The principal environmental consequences arising from the sol-gel process are those associated with the use of strong acids, plasticizers, binders, solvents, and *sec*-butanol formed during the reaction. Depending on the firing conditions, variable amounts of organic materials such as binders and plasticizers may be released as combustion products. NO_x 's may also be produced in the off-gas from residual nitric acid or nitrate salts. Moreover, acids and solvents must be recycled or disposed of. Energy consumption in the process entails "upstream" environmental emissions associated with the production of that energy.

6.5.4.4 Bibliography

- *Advances in Ceramics*, Eds. J. A. Mangels and G. L. Messing, American Ceramic Society, Westville, OH, 1984, Vol. 9.
- Adkins, *J. Am. Chem. Soc.*, 1922, **44**, 2175.
- A. R. Barron, *Comm. Inorg. Chem.*, 1993, **14**, 123.
- M. K. Cinibulk, *Ceram. Eng. Sci., Proc.*, 1994, **15**, 721.
- F. A. Cotton and G. Wilkinson, *Advanced Inorganic Chemistry*, 5th Ed., John Wiley and Sons, New York (1988).
- N. N. Greenwood and A. Earnshaw, *Chemistry of the Elements*, Pergamon Press, Oxford (1984).
- P. H. Hsu and T. F. Bates, *Mineral Mag.*, 1964, **33**, 749.
- W. D. Kingery, H. K. Bowen, and D. R. Uhlmann, *Introduction to Ceramics*, 2nd Ed. Wiley, New York (1976).
- H. Schneider, K. Okada, and J. Pask, *Mullite and Mullite Ceramics*, Wiley (1994).
- R. V. Thomas, *Systems Analysis and Water Quality Management*, McGraw-Hill, New York (1972).
- J. C. Williams, in *Treatise on Materials Science and Technology*, Ed. F. F. Y. Wang, Academic Press, New York (1976).

6.6 Boron Compounds with Nitrogen Donors¹⁰

The "B-N" unit is isoelectronic (3 + 5 valence electrons) to the "C-C" unit (4 + 4 valence electrons). The two moieties are also isolobal, and as such there are many of the compound types formed by carbon have analogous derivatives in the chemistry of boron-nitrogen.

¹⁰This content is available online at <<http://cnx.org/content/m32856/1.2/>>.

6.6.1 Lewis acid-base addition compounds

Boron compounds, BX_3 , are strong Lewis acids and as such form stable addition compounds with Lewis bases, in particular those with nitrogen donor ligands.



In principle these Lewis acid-base complexes should be similar to their isolobal hydrocarbon analogs, however, whereas the dipole in ethane is zero (by symmetry) the dipole in H_3NBH_3 is 5.2 D as a consequence of the difference in the Pauling electronegativities (i.e., B = 2.04 and N = 3.04). It is this dipole that generally differentiates the B-N compounds from their C-C analogs.

Homolytic cleavage of the C-C bond in ethane will yield two neutral methyl radicals, (6.38). In contrast, heterolytic cleavage will result in the formation of two charged species, (6.39). Thus, the products either have a net spin, (6.38), or a net charge, (6.39). By contrast, cleavage of the B-N bond in $\text{H}_3\text{N-BH}_3$ either yields products with both spin and charge, (6.40), or neither, (6.41). Heterolytic cleavage of the B-N bond yields neutral compounds, (6.40), while homolytic cleavage results in the formation of radical ions, (6.41).



The difference in bond strength between $\text{H}_3\text{N-BH}_3$ and ethane is reflected in the difference in bond lengths (Table 6.15).

Compound	Bond length (Å)	Bond strength (kcal/mol)
$\text{H}_3\text{C-CH}_3$	1.533	89
$\text{H}_3\text{N-BH}_3$	1.658	31

Table 6.15: A comparison of bonding in $\text{H}_3\text{E-E}'\text{H}_3$.

6.6.2 Aminoboranes

The group $\text{R}'_2\text{N-BR}_2$ is isoelectronic and isolobal to the olefin sub-unit $\text{R}'_2\text{C=CR}_2$, and there is even appreciable π -bonding character (Figure 6.43). A measure of the multiple bond character can be seen from a comparison of the calculated B-N bond in H_2NBN_2 (1.391 Å) as compared to a typical olefin (1.33 Å). It is interesting that a consideration of the possible resonance form (Figure 6.43) suggest the dipole in the σ -bond is in the opposite direction of that of the π -bond.

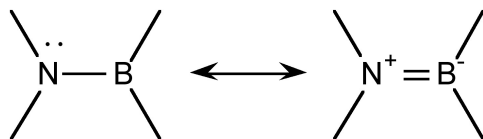


Figure 6.43: Resonance forms for $X_2N-BX'_2$.

Unlike olefins, borazines oligomerize to form dimmers and trimers (Figure 6.44) in the absence of significant steric hindrance. Analogous structures are also observed for the other Group 13-15 homologs ($R_2AlNR'_2$, $R_2GaPR'_2$, etc.).

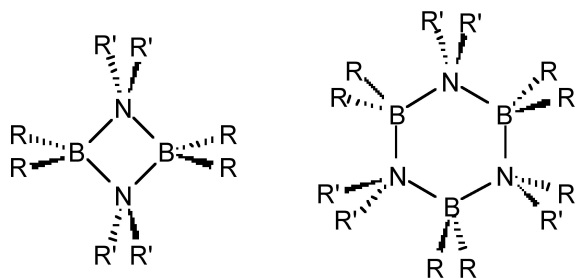
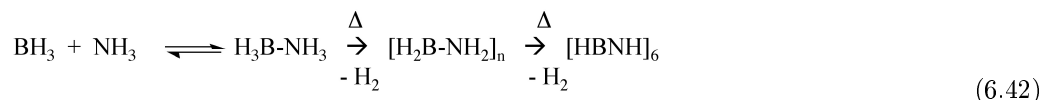


Figure 6.44: Typical structures of aminoboranes.

6.6.3 Borazines

The condensation of boron hydride with ammonia results in the formation of a benzene analog: borazine, (6.42). Substituted derivatives are formed by the reaction with primary amines.



Despite the cyclic structure (Figure 6.45), borazine is not a true analog of benzene. Despite all the B-N bond distances being equal (1.44 Å) consistent with a delocalized structure, the difference in electronegativity of boron and nitrogen (2.04 and 3.04, respectively) results in a polarization of the bonds (i.e., $B^{\delta+}-N^{\delta-}$) and hence a limit to the delocalization. The molecular orbitals of the π -system in borazine are lumpy in appearance (Figure 6.46a) compared to benzene (Figure 6.46b). This uneven distribution makes borazine prone to addition reactions, making it as a molecule less stable than benzene.

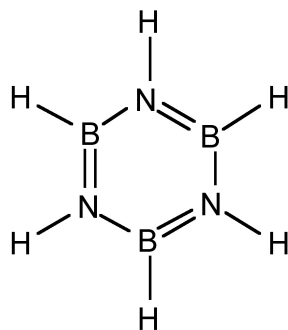


Figure 6.45: Structure of borazine, the inorganic analog to benzene.

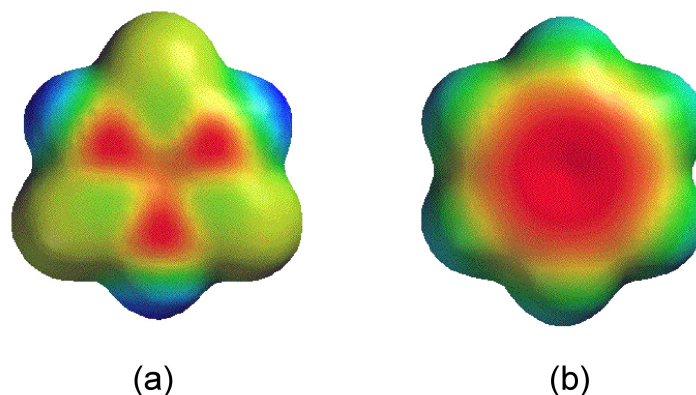


Figure 6.46: Probability distributions for the π -bond orbitals in (a) borazine and (b) benzene.

6.6.3.1 Iminoboranes: analogs of acetylene

Iminoboranes, $\text{RB}=\text{NR}'$, are analogs of alkynes, but like aminoboranes are only isolated as monomers with sterically hindered substituents. In the absence of sufficient steric bulk oligomerization occurs, forming substituted benzene analogs.

6.6.4 Boron nitrides: analogs of elemental carbon

The fusion of borax, $\text{Na}_2[\text{B}_4\text{O}_5(\text{OH})_4]$ with ammonium chloride (NH_4Cl) results in the formation of hexagonal boron nitride (h-BN). Although h-BN has a planar, layered structure consisting of six-member rings similar to graphite (Figure 6.47), it is a white solid. The difference in color is symptomatic of the more localized bonding in BN than in graphite.

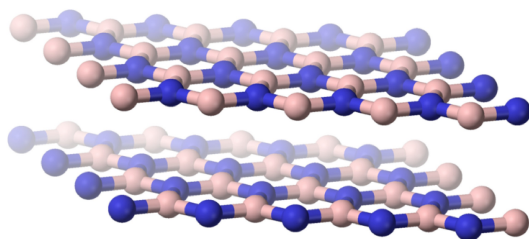


Figure 6.47: Structure of h-BN.

As is found for its carbon analog, hexagonal boron nitride (h-BN or α -BN) is converted at high temperatures (600 – 2000 °C) and pressures (50 – 200 kbar) to a cubic phase (c-BN or β -BN). In a similar manner to diamond, cubic-BN is very hard being actually able to cut diamond, and as a consequence its main use is as an industrial grinding agent. The cubic form has the sphalerite crystal structure (Figure 6.48). Finally, a wurtzite form of boron nitride (w-BN) is known that has similar structure as lonsdaleite, rare hexagonal polymorph of carbon. Table 6.16 shows a comparison of the properties of the hexagonal and cubic phases of BN with their carbon analogs.

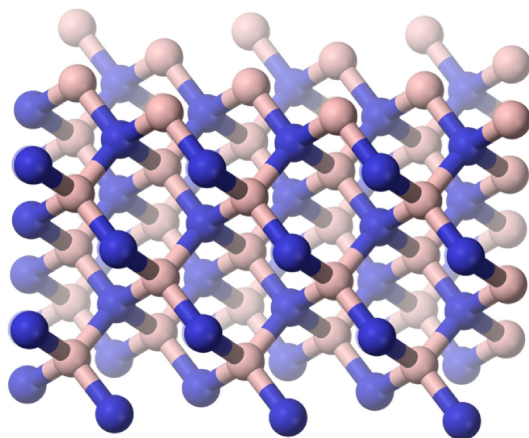


Figure 6.48: Structure of c-BN.

Phase	Carbon	Boron nitride
Cubic	Colorless, hard, mp = 3550 °C. C-C = 1.514 Å	Colorless, hard, B-N = 1.56 Å
Hexagonal	Black solid, planar layers, conductor, mp = 3652 – 3697 °C (sublimes), C-C = 1.415 Å	White solid, planar layers, semiconductor (E _g = 5.2 eV), mp = 2973 °C (sublimes), B-N = 1.45 Å

Table 6.16: Comparison of structural and physical properties of carbon and boron nitride analogs.

The partly ionic structure of BN layers in h-BN reduces covalency and electrical conductivity, whereas the interlayer interaction increases resulting in higher hardness of h-BN relative to graphite.

6.6.5 Bibliography

- K. M. Bissett and T. M. Gilbert, *Organometallics*, 2004, **23**, 850.
- P. Paetzold, *Adv. Inorg. Chem.*, 1987, **31**, 123.
- L. R. Thorne, R. D. Suenram, and F. J. Lovas, *J. Chem. Phys.*, 1983, **78**, 167.

6.7 Gallium Arsenide

6.7.1 Properties of Gallium Arsenide¹¹

6.7.1.1 Gallium: the element

The element gallium was predicted, as eka-aluminum, by Mendeleev in 1870, and subsequently discovered by Lecoq de Boisbaudran in 1875; in fact de Boisbaudran had been searching for the missing element for some years, based on his own independent theory. The first experimental indication of gallium came with the observation of two new violet lines in the spark spectrum of a sample deposited on zinc. Within a month of these initial results de Boisbaudran had isolated 1 g of the metal starting from several hundred kilograms of crude zinc blende ore. The new element was named in honor of France (Latin *Gallia*), and the striking similarity of its physical and chemical properties to those predicted by Mendeleev (Table 6.17) did much to establish the general acceptance of the periodic Law; indeed, when de Boisbaudran first stated that the density of Ga was 4.7 g/cm³ rather than the predicted 5.9 g/cm³, Mendeleev wrote to him suggesting that he redetermine the value (the correct value is 5.904 g/cm³).

Property	Mendeleev's prediction (1871) for eka-aluminum, M	Observed properties of gallium (discovered 1875)
Atomic weight	ca. 68	69.72
Density, g.cm ⁻³	5.9	5.904
Melting point	Low	29.78
<i>continued on next page</i>		

¹¹This content is available online at <<http://cnx.org/content/m22970/1.7/>>.

Vapor pressure	Non-volatile	10^{-3} mmHg, 1000 °C
Valence	3	3
Oxide	M_2O_3	Ga_2O_3
Density of oxide (g/cm^3)	5.5	5.88
Properties of metal	M should dissolve slowly in acids and alkalis and be stable in air	Ga metal dissolves slowly in acids and alkalis and is stable in air
Properties of hydroxide	$M(OH)_3$ should dissolve in both acids and alkalis	$Ga(OH)_3$ dissolves in both acids and alkalis
Properties of salts	M salts will tend to form basic salts; the sulfate should form alums; M_2S_3 should be precipitated by H_2S or $(NH_4)_2S$; anhydrous MCl_3 should be more volatile than $ZnCl_2$	Ga salts readily hydrolyze and form basic salts; alums are known; Ga_2S_3 can be precipitated under special conditions by H_2S or $(NH_4)_2S$, anhydrous $GaCl_3$ is more volatile than $ZnCl_2$.

Table 6.17: Comparison of predicted and observed properties of gallium.

Gallium has a beautiful silvery blue appearance; it wets glass, porcelain, and most other surfaces (except quartz, graphite, and Teflon[®]) and forms a brilliant mirror when painted on to glass. The atomic radius and first ionization potential of gallium are almost identical with those of aluminum and the two elements frequently resemble each other in chemical properties. Both are amphoteric, but gallium is less electropositive as indicated by its lower electrode potential. Differences in the chemistry of the two elements can be related to the presence of a filled set of 3d orbitals in gallium.

Gallium is very much less abundant than aluminum and tends to occur at low concentrations in sulfide minerals rather than as oxides, although gallium is also found associated with aluminum in bauxite. The main source of gallium is as a by-product of aluminum refining. At 19 ppm of the earth's crust, gallium is about as abundant as nitrogen, lithium and lead; it is twice as abundant as boron (9 ppm), but is more difficult to extract due to the lack of any major gallium-containing ore. Gallium always occurs in association either with zinc or germanium, its neighbors in the periodic table, or with aluminum in the same group. Thus, the highest concentrations (0.1 - 1%) are in the rare mineral germanite (a complex sulfide of Zn, Cu, Ge, and As); concentrations in sphalerite (ZnS), bauxite, or coal, are a hundred-fold less.

6.7.1.2 Gallium pnictides

Gallium's main use is in semiconductor technology. For example, GaAs and related compounds can convert electricity directly into coherent light (laser diodes) and is employed in electroluminescent light-emitting diodes (LED's); it is also used for doping other semiconductors and in solid-state devices such as heterojunction bipolar transistors (HBTs) and high power high speed metal semiconductor field effect transistors (MESFETs). The compound $MgGa_2O_4$ is used in ultraviolet-activated powders as a brilliant green phosphor used in Xerox copying machines. Minor uses are as high-temperature liquid seals, manometric fluids and heat-transfer media, and for low-temperature solders.

Undoubtedly the binary compounds of gallium with the most industrial interest are those of the Group 15 (V) elements, GaE ($E = N, P, As, Sb$). The compounds which gallium forms with nitrogen, phosphorus, arsenic, and antimony are isoelectronic with the Group 14 elements. There has been considerable interest, particularly in the physical properties of these compounds, since 1952 when Welker first showed that they had semiconducting properties analogous to those of silicon and germanium.

Gallium phosphide, arsenide, and antimonide can all be prepared by direct reaction of the elements; this is normally done in sealed silica tubes or in a graphite crucible under hydrogen. Phase diagram data is hard to obtain in the gallium-phosphorus system because of loss of phosphorus from the bulk material at elevated

temperatures. Thus, GaP has a vapor pressure of more than 13.5 atm at its melting point; as compared to 0.89 atm for GaAs. The physical properties of these three compounds are compared with those of the nitride in Table 6.18. All three adopt the zinc blende crystal structure and are more highly conducting than gallium nitride.

Property	GaN	GaP	GaAs	GaSb
Melting point (°C)	> 1250 (dec)	1350	1240	712
Density (g/cm ³)	ca. 6.1	4.138	5.3176	5.6137
Crystal structure	Würtzite	zinc blende	zinc blende	zinc blende
Cell dimen. (Å) ^a	$a = 3.187, c = 5.186$	$a = 5.4505$	$a = 5.6532$	$a = 6.0959$
Refractive index ^b	2.35	3.178	3.666	4.388
k (ohm ⁻¹ cm ⁻¹)	$10^{-9} - 10^{-7}$	$10^{-2} - 10^2$	$10^{-6} - 10^3$	6 - 13
Band gap (eV) ^c	3.44	2.24	1.424	0.71

Table 6.18: Physical properties of 13-15 compound semiconductors. ^a Values given for 300 K. ^b Dependent on photon energy; values given for 1.5 eV incident photons. ^c Dependent on temperature; values given for 300 K.

6.7.1.3 Gallium arsenide versus silicon

Gallium arsenide is a compound semiconductor with a combination of physical properties that has made it an attractive candidate for many electronic applications. From a comparison of various physical and electronic properties of GaAs with those of Si (Table 6.19) the advantages of GaAs over Si can be readily ascertained. Unfortunately, the many desirable properties of gallium arsenide are offset to a great extent by a number of undesirable properties, which have limited the applications of GaAs based devices to date.

Properties	GaAs	Si
Formula weight	144.63	28.09
Crystal structure	zinc blende	diamond
Lattice constant	5.6532	5.43095
Melting point (°C)	1238	1415
Density (g/cm ³)	5.32	2.328
Thermal conductivity (W/cm.K)	0.46	1.5
Band gap (eV) at 300 K	1.424	1.12
Intrinsic carrier conc. (cm ⁻³)	1.79×10^6	1.45×10^{10}
Intrinsic resistivity (ohm.cm)	10^8	2.3×10^5
Breakdown field (V/cm)	4×10^5	3×10^5
Minority carrier lifetime (s)	10^{-8}	2.5×10^{-3}
Mobility (cm ² /V.s)	8500	1500

Table 6.19: Comparison of physical and semiconductor properties of GaAs and Si.

6.7.1.3.1 Band gap

The band gap of GaAs is 1.42 eV; resulting in photon emission in the infra-red range. Alloying GaAs with Al to give $\text{Al}_x\text{Ga}_{1-x}\text{As}$ can extend the band gap into the visible red range. Unlike Si, the band gap of GaAs is direct, i.e., the transition between the valence band maximum and conduction band minimum involves no momentum change and hence does not require a collaborative particle interaction to occur. Photon generation by inter-band radiative recombination is therefore possible in GaAs. Whereas in Si, with an indirect band-gap, this process is too inefficient to be of use. The ability to convert electrical energy into light forms the basis of the use of GaAs, and its alloys, in optoelectronics; for example in light emitting diodes (LEDs), solid state lasers (light amplification by the stimulated emission of radiation).

A significant drawback of small band gap semiconductors, such as Si, is that electrons may be thermally promoted from the valence band to the conduction band. Thus, with increasing temperature the thermal generation of carriers eventually becomes dominant over the intentionally doped level of carriers. The wider band gap of GaAs gives it the ability to remain 'intentionally' semiconducting at higher temperatures; GaAs devices are generally more stable to high temperatures than a similar Si devices.

6.7.1.3.2 Carrier density

The low intrinsic carrier density of GaAs in a pure (undoped) form indicates that GaAs is intrinsically a very poor conductor and is commonly referred to as being semi-insulating. This property is usually altered by adding dopants of either the p- (positive) or n- (negative) type. This semi-insulating property allows many active devices to be grown on a single substrate, where the semi-insulating GaAs provides the electrical isolation of each device; an important feature in the miniaturization of electronic circuitry, i.e., VLSI (very-large-scale-integration) involving over 100,000 components per chip (one chip is typically between 1 and 10 mm square).

6.7.1.3.3 Electron mobility

The higher electron mobility in GaAs than in Si potentially means that in devices where electron transit time is the critical performance parameter, GaAs devices will operate with higher response times than equivalent Si devices. However, the fact that hole mobility is similar for both GaAs and Si means that devices relying on cooperative electron and hole movement, or hole movement alone, show no improvement in response time when GaAs based.

6.7.1.3.4 Crystal growth

The bulk crystal growth of GaAs presents a problem of stoichiometric control due the loss, by evaporation, of arsenic both in the melt and the growing crystal ($> ca. 600\text{ }^\circ\text{C}$). Melt growth techniques are, therefore, designed to enable an overpressure of arsenic above the melt to be maintained, thus preventing evaporative losses. The loss of arsenic also negates diffusion techniques commonly used for wafer doping in Si technology; since the diffusion temperatures required exceed that of arsenic loss.

6.7.1.3.5 Crystal Stress

The thermal gradient and, hence, stress generated in melt grown crystals have limited the maximum diameter of GaAs wafers (currently 6" diameter compared to over 12" for Si), because with increased wafer diameters the thermal stress generated dislocation (crystal imperfections) densities eventually becomes unacceptable for device applications.

6.7.1.3.6 Physical strength

Gallium arsenide single crystals are very brittle, requiring that considerably thicker substrates than those employed for Si devices.

6.7.1.3.7 Native oxide

Gallium arsenide's native oxide is found to be a mixture of non-stoichiometric gallium and arsenic oxides and elemental arsenic. Thus, the electronic band structure is found to be severely disrupted causing a breakdown in 'normal' semiconductor behavior on the GaAs surface. As a consequence, the GaAs MISFET (metal-insulator-semiconductor-field-effect-transistor) equivalent to the technologically important Si based MOSFET (metal-oxide-semiconductor-field-effect-transistor) is, therefore, presently unavailable.

The passivation of the surface of GaAs is therefore a key issue when endeavoring to utilize the FET technology using GaAs. Passivation in this discussion means the reduction in mid-gap band states which destroy the semiconducting properties of the material. Additionally, this also means the production of a chemically inert coating which prevents the formation of additional reactive states, which can effect the properties of the device.

6.7.1.4 Bibliography

- S. K. Ghandhi, *VLSI Fabrication Principles: Silicon and Gallium Arsenide*. Wiley-Interscience, New York, (1994).
- *Properties of Gallium Arsenide*. Ed. M. R. Brozel and G. E. Stillman. 3rd Ed. Institution of Electrical Engineers, London (1996).

6.7.2 Electronic Grade Gallium Arsenide¹²

6.7.2.1 Introduction

The synthesis and purification of bulk polycrystalline semiconductor material represents the first step towards the commercial fabrication of an electronic device. This polycrystalline material is then used as the raw material for the formation of single crystal material that is processed to semiconductor wafers.

In contrast to electronic grade silicon (EGS), whose use is a minor fraction of the global production of elemental silicon, gallium arsenide (GaAs) is produced exclusively for use in the semiconductor industry. However, arsenic and its compounds have significant commercial applications. The main use of elemental arsenic is in alloys of Pb, and to a lesser extent Cu, while arsenic compounds are widely used in pesticides and wood preservatives and the production of bottle glass. Thus, the electronics industry represents a minor user of arsenic. In contrast, although gallium has minor uses as a high-temperature liquid seal, manometric fluids and heat transfer media, and for low temperature solders, its main use is in semiconductor technology.

6.7.2.2 Isolation and purification of gallium metal

At 19 ppm gallium (L. *Gallia*, France) is about as abundant as nitrogen, lithium and lead; it is twice as abundant as boron (9 ppm), but is more difficult to extract due to the lack of any major gallium-containing ore. Gallium always occurs in association either with zinc or germanium, its neighbors in the periodic table, or with aluminum in the same group. Thus, the highest concentrations (0.1-1%) are in the rare mineral germanite (a complex sulfide of Zn, Cu, Ge, and As), while concentrations in sphalerite (ZnS), diasporite [AlO(OH)], bauxite, or coal, are a hundred-fold less. Industrially, gallium was originally recovered from the flue dust emitted during sulfide roasting or coal burning (up to 1.5% Ga), however, it is now obtained as side product of vast aluminum industry and in particular from the Bayer process for obtaining alumina from bauxite.

The Bayer process involves dissolution of bauxite, $\text{AlO}_x\text{OH}_{3-2x}$, in aqueous NaOH, separation of insoluble impurities, partial precipitation of the trihydrate, $\text{Al}(\text{OH})_3$, and calcination at 1,200 °C. During processing the alkaline solution is gradually enriched in gallium from an initial weight ratio Ga/Al of about 1/5000 to about 1/300. Electrolysis of these extracts with a Hg cathode results in further concentration, and the solution of sodium gallate thus formed is then electrolyzed with a stainless steel cathode to give Ga metal.

¹²This content is available online at <<http://cnx.org/content/m32000/1.2/>>.

Since bauxite contains 0.003-0.01% gallium, complete recovery would yield some 500-1000 tons per annum, however present consumption is only 0.1% of this about 10 tons per annum.

A typical analysis of the 98-99% pure gallium obtained as a side product from the Bayer process is shown in Table 6.20. This material is further purified to 99.99% by chemical treatment with acids and O₂ at high temperatures followed by crystallization. This chemical process results in the reduction of the majority of metal impurities at the ppm level, see Table 6.20. Purification to seven nines 99.9999% is possible through zone refining, however, since the equilibrium distribution coefficient of the residual impurities $k_0 \approx 1$, multiple passes are required, typically > 500. The low melting point of gallium ensures that contamination from the container wall (which is significant in silicon zone refining) is minimized. In order to facilitate the multiple zone refining in a suitable time, a simple modification of zone refining is employed shown in Figure 6.49. The gallium is contained in a plastic tube wrapped around a rotating cylinder that is half immersed in a cooling bath. A heater is positioned above the gallium plastic coil. Thus, establishing a series of molten zones that pass upon rotation of the drum by one helical segment per revolution. In this manner, 500 passes may be made in relatively short time periods. The typical impurity levels of gallium zone refined in this manner are given in Table 6.20.

Element	Bayer process (ppm)	After acid/base leaching (ppm)	500 zone passes (ppm)
aluminum	100-1,000	7	< 1
calcium	10-100	not detected	not detected
copper	100-1,000	2	< 1
iron	100-1,000	7	< 1
lead	< 2000	30	not detected
magnesium	10-100	1	not detected
mercury	10-100	not detected	not detected
nickel	10-100	not detected	not detected
silicon	10-100	≈ 1	not detected
tin	10-100	≈ 1	not detected
titanium	10-100	1	< 1
zinc	30,000	≈ 1	not detected

Table 6.20: Typical analysis of gallium obtained as a side product from the Bayer process.

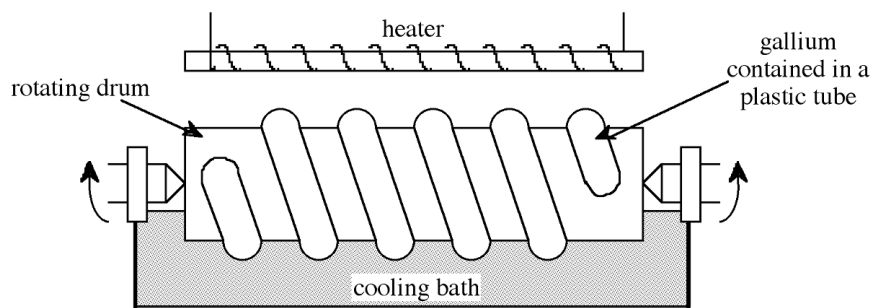


Figure 6.49: Schematic representation of a zone refining apparatus.

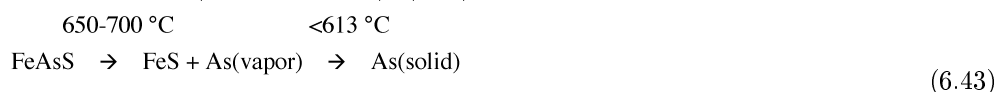
6.7.2.3 Isolation and purification of elemental arsenic

Elemental arsenic (*L. arsenicum*, yellow orpiment) exists in two forms: yellow (cubic, As_4) and gray or metallic (rhombohedral). At a natural abundance of 1.8 ppm arsenic is relatively rare, however, this is offset by its presence in a number of common minerals and the relative ease of isolation. Arsenic containing minerals are grouped into three main classes: the sulfides realgar (As_4S_4) and orpiment (As_2S_3), the oxide arsenolite (As_2O_3), and the arsenides and sulfarsenides of the iron, cobalt, and nickel. Minerals in this latter class include: loellinginite (FeAs_2), saffrolite (CoAs), niccolite (NiAs), rammelsbergite (NiAs_2), ansenopyrite or mispickel (FeAsS), cobaltite (CoAsS), enargite (Cu_3AsS_4), gersdorffite (NiAsS), and the quartunary sulfide glaucodot [$(\text{Co,Fe})\text{AsS}$]. Table 6.21 shows the typical impurities in arsenopyrite.

Element	Concentration (ppm)	Element	Concentration (ppm)
silver	90	nickel	< 3,000
gold	8	lead	50
cobalt	30,000	platinum	0.4
copper	200	rhenium	50
germanium	30	selenium	50
manganese	3,000	vanadium	300
molybdenum	60	zinc	400

Table 6.21: Typical impurities in arsenopyrite.

Arsenic is obtained commercially by smelting either FeAs_2 or FeAsS at 650-700 °C in the absence of air and condensing the sublimed element ($T_{\text{sub}} = 613$ °C), (6.43).



The arsenic thus obtained is combined with lead and then sublimed ($T_{\text{sub}} = 614$ °C) which binds any sulfur impurities more strongly than arsenic. Any residual arsenic that remains trapped in the iron sulfide is separated by forming the oxide (As_2O_3) by roasting the sulfide in air. The oxide is sublimed into the flue system during roasting from where it is collected and reduced with charcoal at 700-800 °C to give elemental arsenic. Semiconductor grade arsenic (> 99.9999%) is formed by zone refining.

6.7.2.4 Synthesis and purification of gallium arsenide.

Gallium arsenide can be prepared by the direct reaction of the elements, (6.44). However, while conceptually simple the synthesis of GaAs is complicated by the different vapor pressures of the reagents and the highly exothermic nature of the reaction. Furthermore, since the synthesis of GaAs at atmospheric pressure is accompanied by its simultaneous decomposes due to the loss by sublimation, of arsenic, the synthesis must be carried out under an overpressure of arsenic in order to maintain a stoichiometric composition of the synthesized GaAs.



In order to overcome the problems associated with arsenic loss, the reaction is usually carried out in a sealed reaction tube. However, if a stoichiometric quantity of arsenic is used in the reaction a constant temperature of 1238 °C must be employed in order to maintain the desired arsenic overpressure of 1 atm. Practically, it is easier to use a large excess of arsenic heated to a lower temperature. In this situation the pressure in the tube is approximately equal to the equilibrium vapor pressure of the volatile component (arsenic) at the lower temperature. Thus, an over pressure of 1 atm arsenic may be maintained if within a sealed tube elemental arsenic is heated to 600-620 °C while the GaAs is maintained at 1240-1250 °C.

Figure 6.50 shows the sealed tube configuration that is typically used for the synthesis of GaAs. The tube is heated within a two-zone furnace. The boats holding the reactants are usually made of quartz, however, graphite is also used since the latter has a closer thermal expansion match to the GaAs product. If higher purity is required then pyrolytic boron nitride (PBN) is used. One of the boats is loaded with pure gallium the other with arsenic. A plug of quartz wool may be placed between the boats to act as a diffuser. The tube is then evacuated and sealed. Once brought to the correct reaction temperatures (Figure 6.50), the arsenic vapor is transported to the gallium, and they react to form GaAs in a controlled manner. Table 6.22 gives the typical impurity concentrations found in polycrystalline GaAs.

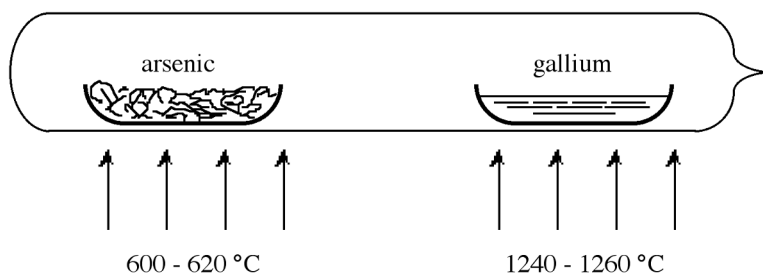


Figure 6.50: Schematic representation of a sealed tube synthesis of GaAs.

Element	Concentration (ppm)	Element	Concentration (ppm)
boron	0.1	silicon	0.02
carbon	0.7	phosphorus	0.1
nitrogen	0.1	sulfur	0.01
oxygen	0.5	chlorine	0.08
fluorine	0.2	nickel	0.04
magnesium	0.02	copper	0.01
aluminum	0.02	zinc	0.05

Table 6.22: Impurity concentrations found in polycrystalline GaAs.

Polycrystalline GaAs, formed from the direct reaction of the elements is often used as the starting material for single crystal growth via Bridgman or Czochralski crystal growth. It is also possible to prepare single crystals of GaAs directly from the elements using in-situ, or direct, compounding within a high-pressure liquid encapsulated Czochralski (HPLEC) technique.

6.7.2.5 Growth of gallium arsenide crystals

When considering the synthesis of Group 13-15 compounds for electronic applications, the very nature of semiconductor behavior demands the use of high purity single crystal materials. The polycrystalline materials synthesized above are, therefore, of little use for 13-15 semiconductors but may, however, serve as the starting material for melt grown single crystals. For GaAs, undoubtedly the most important 13-15 (III - V) semiconductor, melt grown single crystals are achieved by one of two techniques: the Bridgman technique, and the Czochralski technique.

6.7.2.5.1 Bridgman growth

The Bridgman technique requires a two-zone furnace, of the type shown in Figure 6.51. The left hand zone is maintained at a temperature of ca. 610 °C, allowing sufficient overpressure of arsenic within the sealed system to prevent arsenic loss from the gallium arsenide. The right hand side of the furnace contains the polycrystalline GaAs raw material held at a temperature just above its melting point (ca. 1240 °C). As the furnace moves from left to right, the melt cools and solidifies.

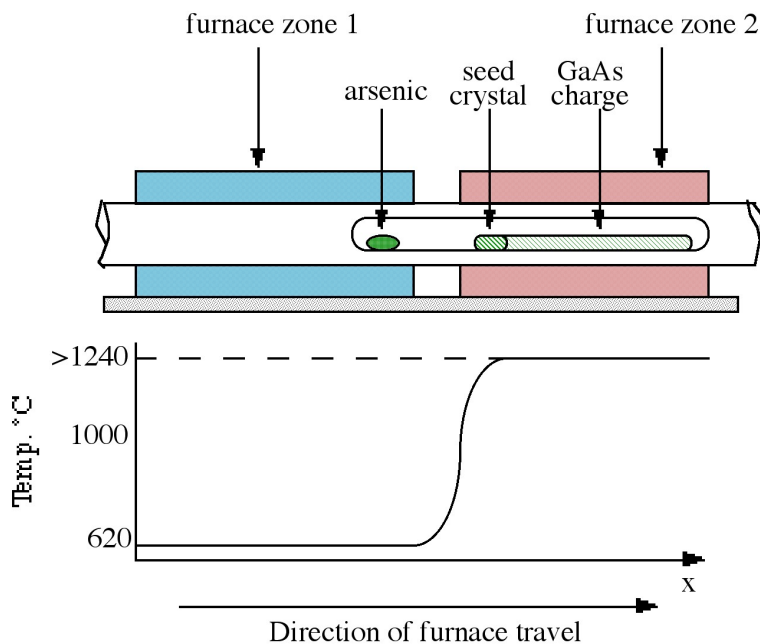


Figure 6.51: A schematic diagram of a Bridgman two-zone furnace used for melt growths of single crystal GaAs.

If a seed crystal is placed at the left hand side of the melt (at a point where the temperature gradient is such that only the end melts), a specific orientation of single crystal may be propagated at the liquid-solid interface eventually to produce a single crystal.

6.7.2.5.2 Czochralski growth

The Czochralski technique, which is the most commonly used technique in industry, is shown in Figure 6.52. The process relies on the controlled withdrawal of a seed crystal from a liquid melt. As the seed is lowered into the melt, partial melting of the tip occurs creating the liquid solid interface required for crystal growth. As the seed is withdrawn, solidification occurs and the seed orientation is propagated into the grown material. The variable parameters of rate of withdrawal and rotation rate can control crystal diameter and purity. As shown in Figure 6.52 the GaAs melt is capped by boron trioxide (B_2O_3). The capping layer, which is inert to GaAs, prevents arsenic loss when the pressure on the surface is above atmospheric pressure. The growth of GaAs by this technique is thus termed liquid encapsulated Czochralski (LEC) growth.

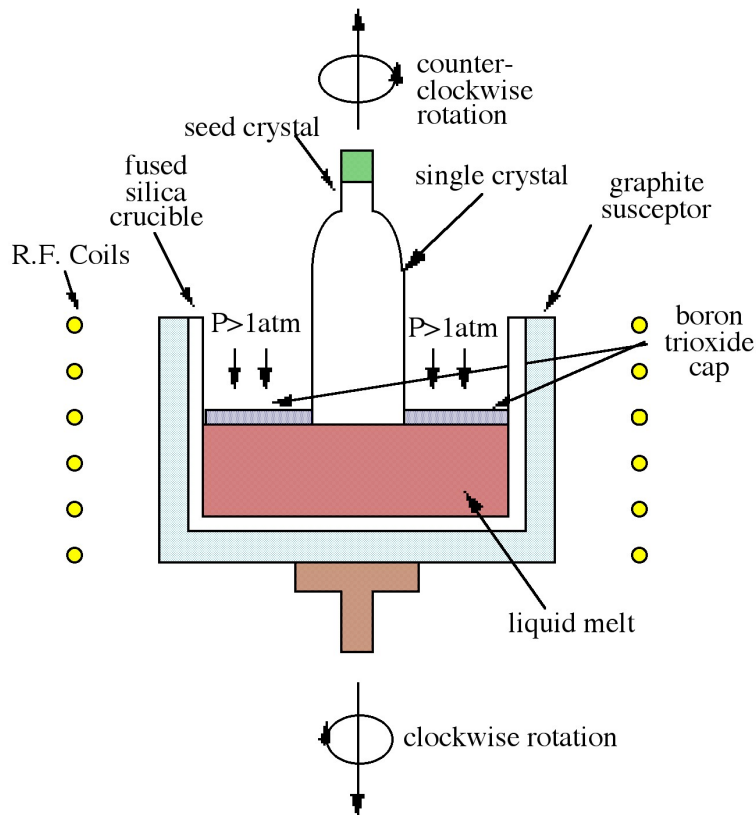


Figure 6.52: A schematic diagram of the Czochralski technique as used for growth of GaAs single crystal bond.

While the Bridgman technique is largely favored for GaAs growth, larger diameter wafers can be obtained by the Czochralski method. Both of these melt techniques produce materials heavily contaminated by the crucible, making them suitable almost exclusively as substrate material. Another disadvantage of these techniques is the production of defects in the material caused by the melt process.

6.7.2.6 Bibliography

- S. K. Ghandhi, *VLSI Fabrication Principles: Silicon and Gallium Arsenide*. Wiley-Interscience, New York, (1994).
- J. Krauskopf, J. D. Meyer, B. Wiedemann, M. Waldschmidt, K. Bethge, G. Wolf, and W. Schültze, *5th Conference on Semi-insulating III-V Materials*, Malmo, Sweden, 1988, Eds. G. Grossman and L. Ledebø, Adam-Hilger, New York (1988).
- W. G. Pfann, *Zone Melting*, John Wiley & Sons, New York (1966).
- R. E. Williams, *Gallium Arsenide Processing Techniques*. Artech House (1984).
- *Properties of Gallium Arsenide*. Ed. M. R. Brozel and G. E. Stillman. 3rd Ed. Institution of Electrical Engineers, London (1996).

6.8 Chalcogenides of Aluminum, Gallium, and Indium¹³

The only stable chalcogenides of aluminum are Al_2S_3 (white), Al_2Se_3 (grey), and Al_2Te_3 (dark grey). They are each prepared by the direct reaction of the elements (100°C) and hydrolyze rapidly in aqueous solution, (6.45). All the chalcogenides have a hexagonal ZnS structure in which $2/3$ of the metal sites are occupied.



The chalcogenides of gallium and indium are more numerous than those of aluminum, and are listed in Table 6.23 and Table 6.24 along with selected physical properties.

Compound	Structural type	Crystallographic system	Cell parameters (\AA , $^\circ$)	Band Gap (eV) ^a
GaS		Hexagonal	$a = 3.587$, $c = 15.492$	3.05 (dir.), 2.593 (ind.)
GaS	ZnS or NaCl	Cubic	$a = 5.5$	4.0 (opt.)
β -GaSe	GaS	Hexagonal	$a = 3.742$, $c = 15.919$	2.103 (dir.), 2.127 (ind.)
γ -GaSe	GaS	Rhombohedral	$a = 3.755$, $c = 23.92$	
δ -GaSe	GaS	Hexagonal	$a = 3.755$, $c = 31.99$	
β -GaTe	GaS	Hexagonal	$a = 4.06$, $c = 16.96$	
GaTe	GaS	Monoclinic	$a = 17.44$, $b = 4.077$, $c = 10.456$, $\beta = 104.4$	1.799 (dir.)
α -Ga ₂ S ₃	Wurtzite	Cubic	$a = 5.181$	
α -Ga ₂ S ₃	Wurtzite	Monoclinic	$a = 12.637$, $b = 6.41$, $c = 7.03$, $\beta = 131.08$	3.438 (opt.)
β -Ga ₂ S ₃	Defect wurtzite	Hexagonal	$a = 3.685$, $c = 6.028$	2.5 - 2.7 (opt.)
α -Ga ₂ Se ₃	Sphalerite	Cubic	$a = 5.429$	2.1 (dir.), 2.04 (ind.)
α -Ga ₂ Te ₃	Sphalerite	Cubic	$a = 5.886$	1.22 (opt.)

Table 6.23: Stoichiometries, structures and selected physical properties of the crystalline chalcogenides of gallium. ^a dir = direct, ind = indirect, opt = optical.

Compound	Structural type	Crystallographic system	Cell parameters (\AA , $^\circ$)	Band gap (eV) ^a
<i>continued on next page</i>				

¹³This content is available online at <<http://cnx.org/content/m33044/1.2/>>.

β -InS	GaS	Orthorhombic	$a = 3.944, b = 4.447, c = 10.648$	2.58 (dir.), 2.067 (ind.)
InS ^b	Hg ₂ Cl ₂	Tetragonal		
InSe	GaS	Rhombohedral	$a = 4.00, c = 25.32$	1.3525 (dir.), 1.32 (ind.)
β -InSe	GaS	Hexagonal	$a = 4.05, c = 16.93$	
InTe	TlSe	Tetragonal	$a = 8.437, c = 7.139$	Metallic
InTe ^b	NaCl	Cubic	$a = 6.18$	
α -In ₂ S ₃	γ -Al ₂ O ₃	Cubic	$a = 5.36$	
β -In ₂ S ₃	Spinel	Tetragonal	$a = 7.618, c = 32.33$	2.03 (dir.), 1.1 (ind.)
α -In ₂ Se ₃	Defect wurtzite	Hexagonal	$a = 16.00, c = 19.24$	
β -In ₂ Se ₃	Defect wurtzite	Rhombohedral	$a = 4.025, c = 19.222$	1.2 - 1.5 (ind.)
α -In ₂ Te ₃	Sphalerite	Cubic	$a = 6.158$	0.92 - 1.15 (opt.)
In ₆ S ₇		Monoclinic	$a = 9.090, b = 3.887, c = 17.705, \beta = 108.20$	0.89 (dir.), 0.7 (ind.)
In ₆ Se ₇	In ₆ S ₇	Monoclinic	$a = 9.430, b = 4.063, c = 18.378, \beta = 109.34$	0.86 (dir.), 0.34 (ind.)
In ₄ Se ₃		Orthorhombic	$a = 15.297, b = 12.308, c = 4.081$	0.64 (dir.)
In ₄ Te ₃	In ₄ Se ₃	Orthorhombic	$a = 15.630, b = 12.756, c = 4.441$	0.48 (dir.)

Table 6.24: Stoichiometries, structures and selected physical properties of the crystalline chalcogenides of indium. ^a dir = direct, ind = indirect, opt = optical. ^b High pressure phase.

The hexagonal β -form of Ga₂S₃ is isostructural with the aluminum analogue; however, while the α -phase was proposed to be hexagonal it was later shown to be monoclinic. A cubic α -phase has been reported. Cubic Sphalerite structures are found for Ga₂Se₃, Ga₂Te₃, and In₂Te₃, in which the structure is based on a cubic close packing of the chalcogenides and the metal atoms occupying $1/3$ of the tetrahedral sites. These structures are all formed with rapid crystallization; slow crystallization and/or thermal annealing leads to ordering and the formation of more complex structures. The indium sulfides, and selenides derivatives are spinel (γ -Al₂O₃), and defect Würtzite, respectively.

Unlike the chalcogenides of aluminum, those of gallium and indium also form subvalent compounds, i.e., those in which the metal is formally of an oxidation state less than +3. Of these subvalent chalcogenides the (formally) divalent materials are of the most interest. The thermodynamically stable phase of GaS has a hexagonal layer structure (Figure 6.53) with Ga-Ga bonds (2.48 Å). The compound can, therefore, be considered as an example of Ga(II). Each Ga is coordinated by three sulfur atoms and one gallium, and the sequence of layers along the z-axis is \cdots S-Ga-Ga-S \cdots S-Ga-Ga-S \cdots .

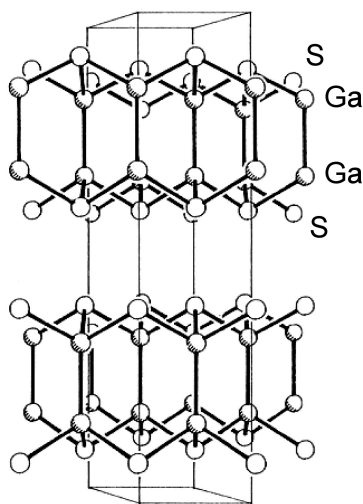


Figure 6.53: The $\cdots\text{S-Ga-Ga-S}\cdots\text{S-Ga-Ga-S}\cdots$ structure of hexagonal GaS. Gallium atoms are shown shaded.

The structures of β -GaSe, and β -InSe are similar to hexagonal GaS. The layered structure of GaTe is similar in that it consists of $\cdots\text{TeGaGaTe}\cdots$ layers, but is monoclinic, while InS is found in both a (high pressure) tetragonal phase (Figure 6.54a) as well as an orthorhombic phase (Figure 6.54b). By contrast to these M-M bonded layered compounds InTe (Figure 6.55) has a structure formalized as $\text{In(I)}[\text{In(III)Te}_2]$; each In(III) is tetrahedrally coordinated to four Te and these tetrahedra are linked *via* shared edges; the In(I) centers lying between these chains.

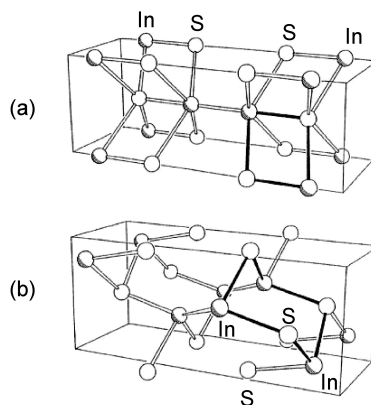


Figure 6.54: Unit cell of (a) tetragonal InS and (b) orthorhombic InS. Indium atoms are shown shaded, and the solid bonds represent the smallest cyclic structural fragment.

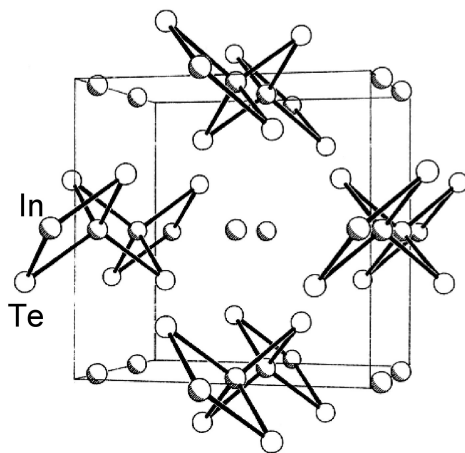


Figure 6.55: Unit cell of tetragonal InTe. Indium atoms are shown shaded, and the solid bonds represent the $[\text{InTe}_2]_{\infty}$ chains.

Further sub-chalcogenides are known for indium, e.g.; In_4Se_3 , which contains $[\text{In}(\text{III})_3\text{Se}_2]^{5+}$ groups (Figure 6.56). While the formally In(I) molecule In_2S has been detected in the gas phase, it is actually a mixture of In and InS in the solid state.

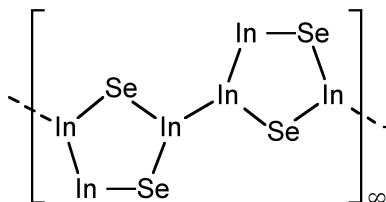


Figure 6.56: Structure of $[\text{In}(\text{III})_3\text{Se}_2]^{5+}$ groups in In_4Se_3 .

6.8.1 Bibliography

- W. J. Duffin and J. H. C. Hogg, *Acta Crystallogr.*, 1966, **20**, 566.
- J. Goodyear and G. Steigman, *Acta Crystallogr.* 1963, **16**, 946.
- H. Hahn and G. Frank, *Z. Anorg. Allgem. Chem.*, 1955, **278**, 340.
- S. Kabalkina, V. G. Losev, and N. M. Gasanly, *Solid State Commun.*, 1982, **44**, 1383.
- A. Keys, S. G. Bott, and A. R. Barron, *Chem. Mater.*, 1999, **11**, 3578.
- A. N. MacInnes, M. B. Power, and A. R. Barron, *Chem. Mater.*, 1992, **4**, 11.
- A. N. MacInnes, W. M. Cleaver, A. R. Barron, M. B. Power, and A. F. Hepp, *Adv. Mater. Optics. Electron.*, 1992, **1**, 229.
- K. Schubert, E. Dörre, and E. Günzel, *Naturwissenschaften*, 1954, **41**, 488.

6.9 Group 13 Halides¹⁴

6.9.1 Trihalides, MX_3

As shown in Table 6.25 all the combinations of Group 13 element (M) and halogen (X) exist for the trihalides (MX_3), except thallium(III) iodide. It should be noted that while there is a compound with the general formula TlI_3 , it is actually a thallium(I) compound of I_3^- .

¹⁴This content is available online at <http://cnx.org/content/m35210/1.1/>.

Element	Mp (°C)	Bp (°C)
BF ₃	-126.8	-100.3
BCl ₃	-107.3	12.6
BBr ₃	-46.3	91.3
BI ₃	49.9	210
AlF ₃	1291	-
AlCl ₃	192.4 (anhydrous), 0.0 (hexahydrate)	120 (hexahydrate)
AlBr ₃	97.8	265
AlI ₃	189.4 (anhydrous) 185 dec. (hexahydrate)	300 subl.
GaF ₃	800	1000
GaCl ₃	77.9	201
GaBr ₃	121.5	278.8
GaI ₃	212	345
InF ₃	1172	-
InCl ₃	586	800
InBr ₃	220	-
InI ₃	210 subl.	-
TlF ₃	300 dec.	-
TlCl ₃	40 dec.	-
TlBr ₃	40 dec.	-

Table 6.25: Selected physical properties of the Group 13 trihalides, MX₃.

The trihalides of boron are all monomers with a coordination number of 3 (Table 6.26), as evidence from their low melting points (Table 6.25). In contrast, the fluorides and chlorides of the heavier Group 13 elements (except GaCl₃) are generally ionic or have a high ionic character, with a coordination number of 6 (Table 6.26, Figure 6.57 and Figure 6.58). The bromides and iodides (except InBr₃) are generally dimeric with a coordination number of 4 (Table 6.26) and have molecular structures involving halide bridging ligands (Figure 6.59 and Table 6.27). AlCl₃ is unusual in that in the solid state it has an ionic structure, but it is readily sublimed, and in the vapor phase (and liquid phase) it has a dimeric structure (Figure 6.59).

Element	Fluoride	Chloride	Bromide	Iodide
B	3	3	3	3
Al	6	6 (4)	4	4
Ga	6	4	4	4
In	6	6	6	4
Tl	6	6	4	-

Table 6.26: The Group 13 element coordination numbers for the trihalides, MX₃.

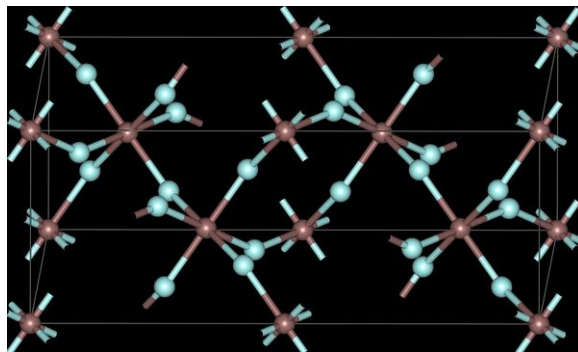


Figure 6.57: Solid state structure of MF_3 ($M = \text{Al, Ga, In}$). Grey spheres represent the metal, while pale blue spheres represent fluorine.

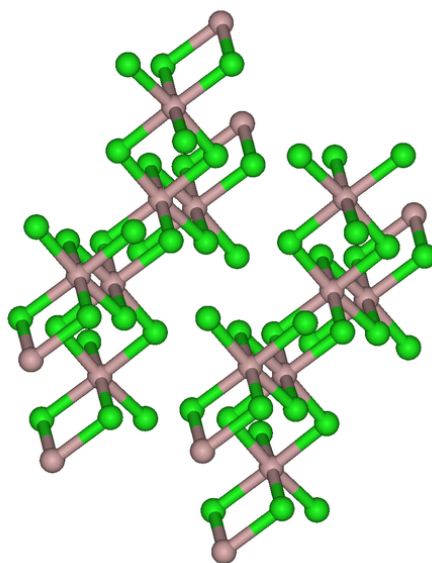


Figure 6.58: Solid state structure of MCl_3 ($M = \text{Al, In, Tl}$) and MBr_3 ($M = \text{In}$). Grey spheres represent the metal, while green spheres represent the halogen.

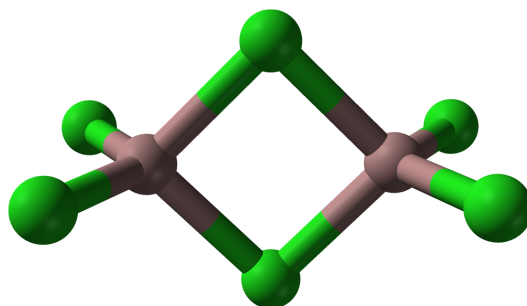


Figure 6.59: Structure of GaCl_3 , MBr_3 ($\text{M} = \text{Al, Ga, Tl}$), and MI_3 ($\text{M} = \text{Al, Ga, In}$). Grey spheres represent the metal, while green spheres represent the halogen.

Compound	M-X_t (\AA) ^a	M-X_b (\AA) ^a	$\text{X}_t\text{-M-X}_t$ ($^\circ$) ^a	$\text{X}_b\text{-M-X}_b$ ($^\circ$) ^a	M-X-M ($^\circ$)
Al_2Br_6	2.21	2.33	115	93	87
In_2I_6	2.64	2.84	125.1	93.7	86.3

Table 6.27: Selected bond lengths and angles for dimeric M_2X_6 compounds. ^a X_t and X_b indicate terminal and bridging halides, respectively.

6.9.1.1 Synthesis

Boron trifluoride (BF_3) is manufactured commercially by the reaction of boron oxides with hydrogen fluoride, (6.46). The HF is produced *in-situ* from sulfuric acid and fluorite (CaF_2). On smaller scales, BF_3 is prepared by the thermal decomposition of diazonium salts, (6.47).

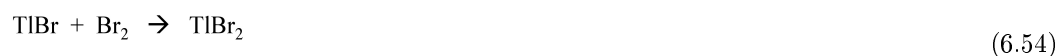


Boron trichloride is also made from boron oxide, but in the presence of carbon, (6.48).



Many of the trihalides are readily prepared by either the direct reaction of the metal with the appropriate halogen, (6.49) - (6.51), or the acid, (6.52) and (6.53). Thallium tribromide can be prepared in CH_3CN by treating a solution of the monobromide with bromine gas, (6.54).





6.9.1.2 Reactivity

The reaction chemistry of the Group 13 trihalides tends to fall into two categories:

- Lewis acid-base complex formation.
- Hydrolysis.

There are, however, a number of reactions involving halide exchange reactions. Aluminum tribromide reacts with carbon tetrachloride at 100 °C to form carbon tetrabromide, (6.55), and with phosgene yields carbonyl bromide and aluminum chlorobromide, (6.56).



Group 13 halides are used as synthons for their organometallic derivatives, (6.57) and (6.58).



6.9.1.2.1 Lewis acid-base complexes

All of the trihalides are strong Lewis acids, and as such react with Lewis base compounds to form Lewis acid-base complexes, (6.59). The extent of the equilibrium is dependant on the Lewis acidity of the trihalide and the basicity of the Lewis base. For example, with BCl_3 , oxygen donor ligands result in approximately 50:50 ratio of BCl_3 and BCl_3L , while for nitrogen donor ligands the equilibrium is shifted to the formation of the complex.



The general structure of the Lewis acid-base complexes is such that the Group 13 element is close to tetrahedral (Figure 6.60). However, for aluminum and the heavier Group 13 elements, more than one ligand can coordinate (Figure 6.61) up to a maximum of six.

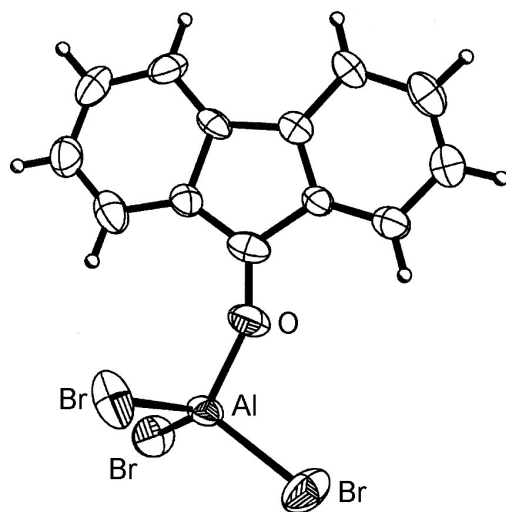


Figure 6.60: Molecular structure of a typical Group 13 metal trihalide Lewis acid-base complex: AlBr₃(9-fluorenone). Adapted from C. S. Branch, S. G. Bott, and A. R. Barron, *J. Organomet. Chem.*, 2003, **666**, 23.

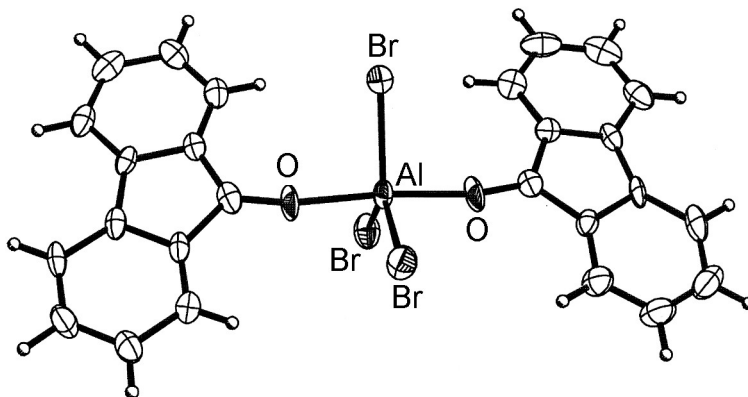


Figure 6.61: Molecular structure of AlBr₃(9-fluorenone)₂. Adapted from C. S. Branch, S. G. Bott, and A. R. Barron, *J. Organomet. Chem.*, 2003, **666**, 23.

It should be noted that the dimeric form of MX₃ (Figure 6.59) can be thought of as mutual Lewis acid-base complexes, in which a Lewis basic lone pair of a halide on one MX₃ unit donates to the Lewis acidic metal on another MX₃ unit.

6.9.1.2.2 Hydrolysis

Generally the fluorides are insoluble in water while the heavier halides are more soluble. However, BF_3 , BCl_3 , and BBr_3 all decompose in the presence of water, (6.60). In the case of the fluoride, the HF formed reacts with BF_3 to form fluoroboric acid, (6.61). However, there is also a minor equilibrium (2-3%) resulting in the formation of the BF_3 complex of OH^- and H_3O^+ , (6.62).



While the boron compounds (and AlBr_3) decompose even in moist air, AlCl_3 reacts more slowly to make aluminum chlorohydrate (ACH) which has the general formula $\text{Al}_n\text{Cl}_{3n-m}(\text{OH})_m$. While ACH has been proposed to exist as a number of cluster species, it is actually a range of nanoparticles.

ACH is also known as polyaluminum chloride (PAC). The latter name is often used in water purification, where ACH is preferred over alum derivatives ($\text{Al}_2(\text{SO}_4)_3$). The combination of ACH and a high molecular weight quaternized ammonium polymer (e.g., diallyl dimethyl ammonium chloride (DADMAC)), has been known as an effective combination as a flocculant in water treatment process to remove dissolved organic matter and colloidal particles present in suspension.

Aluminum chlorohydrate (ACH) and aluminum-zirconium compounds, are frequently used as the active ingredient in antiperspirants. The mode of action of most aluminum-based compounds involves the dramatic change in the particle size from nano to micro as a function of pH and electrolyte changes on the skin (as compared to the antiperspirant stick or suspension) and hence forming a gel plug in the duct of the sweat gland. The plugs prevent the gland from excreting liquid and are removed over time by the natural sloughing of the skin. A further mechanism of action involves the absorption of 3-methyl-2-hexenoic acid (Figure 6.62). Human perspiration is odorless until bacteria ferment it. Bacteria thrive in hot, humid environments such as the underarm. When adult armpits are washed with alkaline pH soaps, the skin loses its acid mantle (pH = 4.5 - 6), raising the skin pH and disrupting the skin barrier. The bacteria thrive in the basic environment, and feed on the sweat from the apocrine glands and on dead skin and hair cells, releasing 3-methyl-2-hexenoic acid, which is the primary cause of body odor. As with all carboxylic acids, 3-methyl-2-hexenoic acid, reacts in a facile manner with the surface of the alumina nanoparticles. Aluminum chloride salts also have a slight astringent effect on the pores; causing them to contract, further preventing sweat from reaching the surface of the skin.

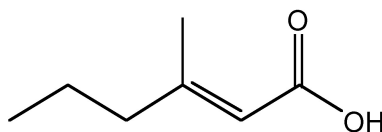


Figure 6.62: The structure of 3-methyl-2-hexenoic acid.

6.9.1.3 Boron trihalides: a special case

The three lighter boron trihalides, BX_3 ($\text{X} = \text{F}, \text{Cl}, \text{Br}$) form stable adducts with common Lewis bases. Their relative Lewis acidities can be evaluated in terms of the relative exothermicity of the adduct-forming reaction:



This trend is opposite to that expected based upon the electronegativity of the halogens. The best explanation of this trend takes into account the extent of π -donation that occurs between the filled lone pair orbital on the halogens and the empty p-orbital on the planar boron (Figure 6.63). As such, the greater the π -bonding the more stable the planar BX_3 configuration as opposed to the pyramidalization of the BX_3 moiety upon formation of a Lewis acid-base complex, (6.59).

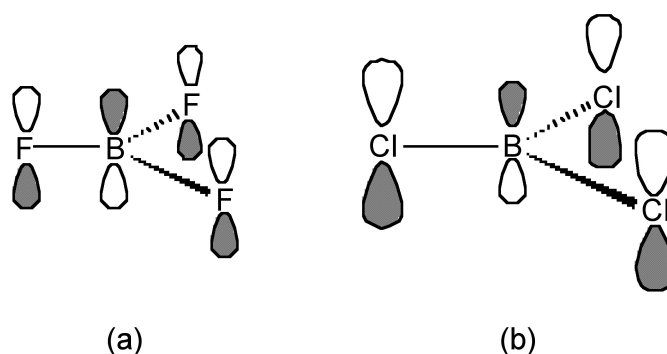


Figure 6.63: Schematic representation of π -donation from filled halogen p-orbitals into empty p-orbital in the halides BX_3 .

The criteria for evaluating the relative strength of π -bonding are not clear, however, one suggestion is that the F atom is small compared to the Cl atom, and the lone pair electron in p_z of F is readily and easily donated and overlapped to empty p_z orbital of boron (Figure 6.63a). In contrast, the overlap for the large (diffuse) p-orbitals on the chlorine is poorer (Figure 6.63b). As a result, the π -donation of F is greater than that of Cl. Interestingly, as may be seen from Table 6.28, any difference in B-X bond length does not follow the expected trend associated with shortening of the B-X bond with stronger π -bonding. In fact the B-Br distance is the most shortened as compared to that expected from the covalent radii (Table 6.28).

Compound	B-X (\AA)	X covalent radius (\AA)	Sum of covalent radii (\AA) ^a	Δ (\AA)
BF_3	1.313	0.57(3)	1.41	0.097
BCl_3	1.75	1.02(4)	1.86	0.11
BBr_3	1.898	1.20(3)	2.04	0.142
BI_3	2.125	1.39(3)	2.23	0.105

Table 6.28: The B-X bond distances in the boron trihalides, BX_3 , as compared to the sum of the covalent radii. ^aCovalent radius of B = 0.84(3) \AA .

At the simplest level the requirements for bonding to occur based upon the molecular or atomic orbital are:

- Directional relationship of the orbitals.
- Relative symmetry of the orbitals.
- Relative energy of the orbitals.
- Extent of orbital overlap

In the case of the boron trihalides, the direction (parallel) and symmetry (p-orbitals) are the same, and the only significant difference will be the relative energy of the donor orbitals (i.e., the lone pair on the halogen) and the extent of the overlap. The latter will be dependant on the B-X bond length (the shorter the bond the greater the potential overlap) and the diffusion of the orbitals (the less diffuse the orbitals the better the overlap). Both of these factors will benefit B-F over B-Cl and B-Br. Thus, the extent of potential overlap would follow the order: (6.63). Despite these considerations, it is still unclear of the exact details of the rationalization of the low Lewis basicity of BF_3 as compared to BCl_3 and BBr_3 .

6.9.1.4 Anionic halides

The trihalides all form Lewis acid-base complexes with halide anions, (6.64), and as such salts of BF_4^- , AlCl_4^- , GaCl_4^- , and InCl_4^- are common.



In the case of gallium the Ga_2Cl_7^- anion (Figure 6.64) is formed from the equilibrium:

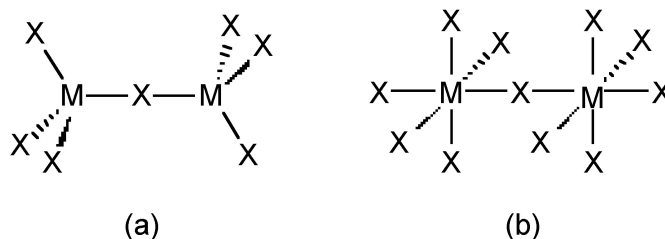


Figure 6.64: Structures of the (a) M_2X_7^- and (b) $\text{M}_2\text{X}_9^{3-}$ anions.

As a consequence of its larger size indium forms a wide range of anionic halides addition compounds with trigonal bipyramidal, square pyramidal, and octahedral coordination geometries. For example, salts of InCl_5^{2-} , InBr_5^{2-} , InF_6^{3-} , InCl_6^{3-} and InBr_6^{3-} have all been made. The InCl_5^{2-} ion has been found to be square pyramidal in the salt $[\text{NEt}_4]_2\text{InCl}_5$, but is trigonal bipyramidal in the acetonitrile solvate of $[\text{Ph}_4\text{P}]_2\text{InCl}_5$. The oligomeric anionic halides In_2X_7^- and $\text{In}_2\text{X}_9^{3-}$ ($\text{X} = \text{Cl}$ and Br) contain binuclear anions with tetrahedral and octahedrally coordinated indium atoms, respectively (Figure 6.64).

6.9.2 Low valent halides

6.9.2.1 Oxidation state +2

Boron forms a series of low oxidation halides containing B-B bonds a formal oxidation state of +2. Passing an electric discharge through BCl_3 using mercury electrodes results in the synthesis of B_2Cl_4 , (6.66). An

alternative route is by the co-condensation of copper as a reducing agent with BCl_3 , (6.67).



B_2F_4 has a planar structure (Figure 6.65) with D_{2h} symmetry, while B_2Cl_4 has the same basic structure it has a staggered geometry (Figure 6.66). The energy for bond rotation about the B-B bond is very low (5 kJ/mol) that can be compared to ethane (12.5 kJ/mol). The bromide, B_2Br_4 , is also observed to be staggered in the solid state. The staggered conformation is favorable on steric grounds, however, for B_2F_4 the planar geometry is stabilized by the smaller size of the halide, and more importantly the presence of strong delocalized π -bonding.

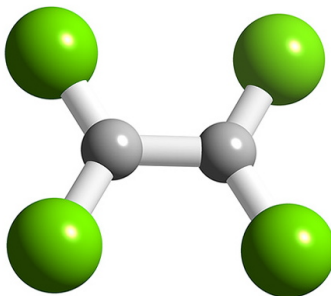


Figure 6.65: The planar structure of B_2F_4 .

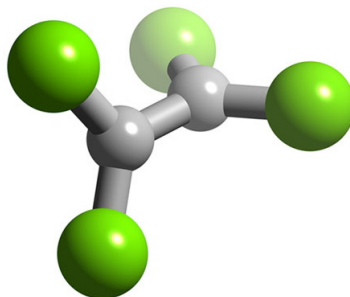


Figure 6.66: The staggered structure of B_2Cl_4 .

6.9.2.2 Oxidation state +1

Boron forms a number of halides with cluster structures, $B_n Cl_n$ where $n = 4$ (Figure 6.67), 8, 9, 10, 11, and 12. Each compound is made by the decomposition of $B_2 Cl_4$. For gallium, none of the monohalides are stable at room temperature, but $GaCl$ and $GaBr$ have been produced in the gas form from the reaction of HX and molten gallium. The stability of thallium(I) as compared to thallium(III) results in the monohalides, $TlCl$, $TlBr$, and TlI being stable. Each compound is insoluble in water, and photosensitive.

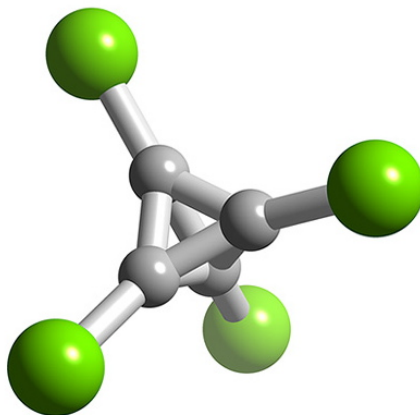


Figure 6.67: Structure of $B_4 Cl_4$.

6.9.3 Intermediate halides

The dihalides (MX_2) of gallium, indium, and thallium do not actually contain the metal in the +2 oxidation state. Instead they are actually mixed valence compound, i.e., $M^+ [MX_4]^-$. The dihalides of gallium are unstable in the presence of water disproportionating to gallium metal and gallium(III) entities. They are soluble in aromatic solvents, where arene complexes have been isolated and the arene is η^6 -coordinated to the Ga^+ ion. $InBr_2$ and InI_2 are greenish and yellow crystalline solids, respectively, which are formulated $In(I)[In(III)X_4]$. $TlCl_2$ and $TlBr_2$ both are of similar formulations.

$Ga_2 X_3$ ($X = Br, I$) and $In_2 Br_3$ are formulated $M(I)_2 [M(II)_2 X_6]$. Both anions contain a M-M bond where the metal has a formal oxidation state of +2. The $Ga_2 Br_6^{2-}$ anion is eclipsed like the $In_2 Br_6^{2-}$ anion, whereas the $Ga_2 I_6^{2-}$ anion is isostructural with $Si_2 Cl_6$ with a staggered conformation. $In_2 Cl_3$ is colorless and is formulated $In(I)_3 [In(III)Cl_6]$.

$Ga_3 Cl_7$ contains the $Ga_2 Cl_7^-$ ion, which has a structure similar to the dichromate, $Cr_2 O_7^{2-}$, ion with two tetrahedrally coordinated gallium atoms sharing a corner (Figure 6.68). The compound can be formulated as gallium(I) heptachlorodigallate(III), $Ga(I)[Ga(III)_2 Cl_7]$.

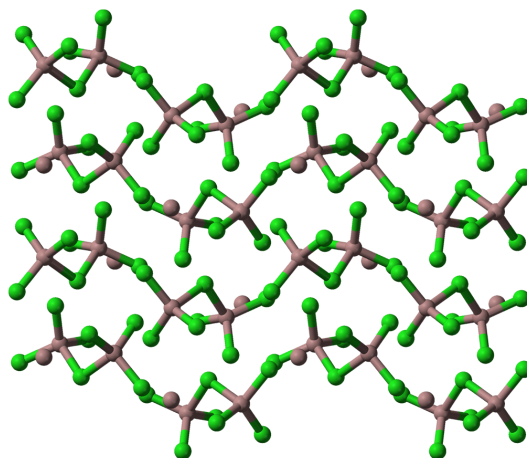


Figure 6.68: The crystal structure of Ga_3Cl_7 , better described as gallium(I) heptachlorodigallate(III), $\text{Ga(I)[Ga(III)}_2\text{Cl}_7]$. Grey spheres represent the gallium, while green spheres represent the chlorine.

In_4Br_7 is light sensitive (like TlCl and TlBr) decaying to InBr_2 and In metal. It is a mixed salt containing the InBr_4^- and InBr_6^{3-} anions balanced by In^+ cations. It is formulated $\text{In(I)}_5[\text{In(III)Br}_4]_2[\text{In(III)Br}_6]$. In_5Br_7 is a pale yellow solid formulated as $\text{In(I)}_3[\text{In(II)}_2\text{Br}_6]\text{Br}$. The $\text{In(II)}_2\text{Br}_6^{2-}$ anion has an eclipsed ethane like structure with an In-In bond length of 2.70 Å. In_5Cl_9 is formulated $\text{In(I)}_3[\text{In(III)}_2\text{Cl}_9]$, with the $\text{In}_2\text{Cl}_9^{2-}$ anion having two 6 coordinate indium atoms with 3 bridging chlorine atoms, face sharing bioctahedra. Finally, In_7Cl_9 and In_7Br_9 have a structure formulated as $\text{InX}_6[\text{In(III)X}_6]\text{X}_3$.

6.9.4 Bibliography

- P. M. Boorman and D. Potts, *Can. J. Chem.*, 1974, **52**, 2016.
- A. Borovik and A. R. Barron, *J. Am. Chem. Soc.*, 2002, **124**, 3743.
- A. Borovik, S. G. Bott, and A. R. Barron, *J. Am. Chem. Soc.*, 2001, **123**, 11219.
- C. S. Branch, S. G. Bott, and A. R. Barron, *J. Organomet. Chem.*, 2003, **666**, 23.
- W. M. Brown and M. Trevino, *US Patent* 5,395,536 (1995).
- S. K. Dentel, *CRC Critical Reviews in Environmental Control*, 1991, **21**, 41.
- D. E. Hassick and J. P. Miknevich, *US Patent* 4,800,039 (1989).
- M. D. Healy, P. E. Laibinis, P. D. Stupik and A. R. Barron, *J. Chem. Soc., Chem. Commun.*, 1989, 359.
- K. Hedberg and R. Ryan, *J. Chem. Phys.*, 1964, **41**, 2214.
- Y. Koide and A. R. Barron, *Organometallics*, 1995, **14**, 4026.
- G. Santiso-Quiñones and I. Krossing, *Z. Anorg. Allg. Chem.*, 2008, **634**, 704.

Solutions to Exercises in Chapter 6

Solution to Exercise 6.4.2.1 (p. 230)

1. Total number of valence electrons = $(6 \times \text{B}) + (3 \times \text{H}) = (6 \times 3) + (6 \times 1) + 2 = 26$
2. Number of electrons for each B-H unit = $(6 \times 2) = 12$
3. Number of skeletal electrons = $26 - 12 = 14$
4. Number SEP = $14/2 = 7$
5. If $n+1 = 7$ and n boron atoms, then $n = 6$
6. Structure of $n = 6$ is octahedral (Figure 6.28), therefore $\text{B}_6\text{H}_6^{2-}$ is a *closo* structure based upon an octahedral structure (Figure 6.69).

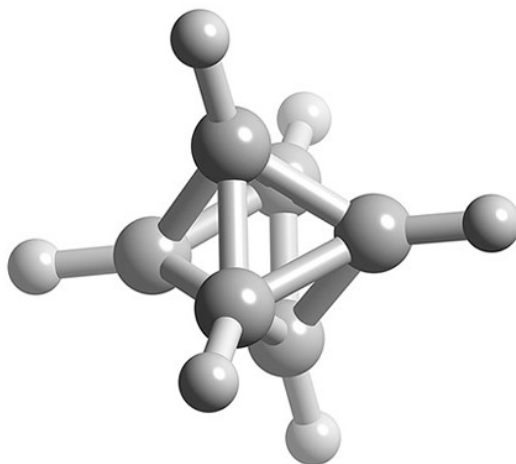


Figure 6.69: Ball and stick representation of the structure of $\text{B}_6\text{H}_6^{2-}$.